FOM-r_d Plane: An Effective Design and Analysis Methodology for Resonant Energy Link in Inductive Power Transfer

Chae-Ho Jeong, Hee-Su Choi, and Sung-Jin Choi, *Member, IEEE*
School of Electrical Engineering
University of Ulsan
Ulsan, Korea
{cogh6253, chs1020}@mail.ulsan.ac.kr, sjchoi@ulsan.ac.kr

***Abstract*— Resonant energy link plays a vital role in the performance of inductive wireless power transfer (IPT) system, whereas the effective design method has not been actively investigated from a perspective of power conversion circuit. This paper presents a new graphical design method based on FOM-r_d plane which gives convenience as well as insight to circuit designers. The proposed FOM-r_d plane can estimate the voltage gain and efficiency according to the variations of magnetic coupling coefficient and the load resistance. Furthermore, the gain bifurcation phenomenon which hampers soft-switching operation and complicates the output voltage control can be readily avoided from the operating region. An energy link for 200 W wireless power transfer system in series-series configuration has been designed and constructed by the proposed method, and its hardware test result verifies the usefulness of the proposed method.**

***Index Terms*—Inductive power transfer, figure of merit, design plane analysis, S-S configuration.**

I. Introduction

Inductive wireless power transfer (IPT) technology improves both safety and convenience and enables waterproofing by removing the metal contacts. Generally, IPT utilizes Faraday induction between two adjacent magnetically coupled coils located apart. In order to increase the power transfer efficiency in a mid-range application, the coils are compensated by capacitors in series or parallel, which constitute a pair of resonant energy link structure [1] - [3]. Such a resonant structure can be categorized into series-series (S-S), series-parallel (S-P), parallel-series (P-S), and parallel-parallel (P-P) configurations in Fig. 1, and a typical IPT system in S-S configuration is described in Fig. 2.

It goes without saying that design of the resonant energy link structure is important because it determines the overall performance of wireless power transfer [4]. Many researchers have studied the resonant energy transfer mechanism. However, only a few systematic design methods has been thoroughly investigated from a perspective of power conversion circuit. The theoretical approach based on coupling theory in [5] only focuses on the resonant link, and the efficiency is represented

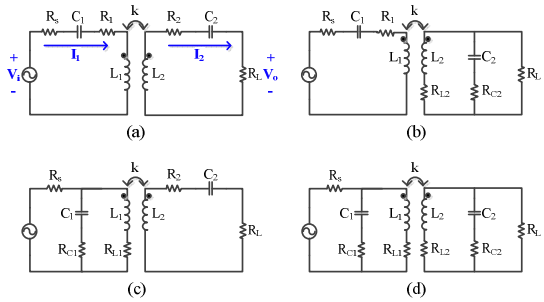

Fig. 1. A resonant structures in IPT. (a) S-S (b) S-P (c) P-S and (d) P-P.

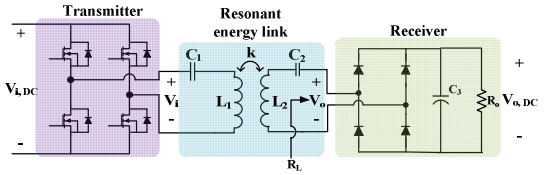

Fig. 2. A typical IPT system in S-S configuration.

by scattering parameters that are unfamiliar to power electronics engineers. In [6], more circuit-friendly design procedure has been suggested. However, the design equations are too complex to use and thus it is very difficult to estimate the performance according to the variations of the load resistance and the magnetic coupling coefficient caused by perturbations in coil alignment or distance. In [7] a systematic design considering both energy link efficiency and voltage gain has the advantage of constant voltage gain regardless of load, but it does not take the change of voltage gain into account when the coupling coefficient variation changes.

This paper presents a new graphical design method based on FOM-r_d plane which gives convenience as well as design insight to circuit engineers. A theoretical formulation is to be presented and followed by hardware verification to check validity and effectiveness of the proposed method.

II. The Proposed Design Plane

A. Theoretical Derivation

Fig. 1 (a) is the AC equivalent circuit of the IPT system. In the figure, V_i, I_1, and I_2 are the phasor representations of the input voltage, the transmitter (Tx) current, the receiver (Rx)

TABLE I
NOMENCLATURES

Symbol	Quantity
L_1, L_2	self-inductances of Tx and Rx resonator
C_1, C_2	compensation capacitors for Tx and Rx resonator magnetic induction
R_1, R_2	total ESR's for Tx and Rx resonator
R_s	internal resistance of the voltage source
R_L	equivalent load resistance
k_1, k_2	coupling coefficients
k	geometric mean of k_1 and k_2
ω	operating angular frequency
ω_o	resonant angular frequency of resonator
Z_{o1}, Z_{o2}	characteristic impedances of Tx and Rx $Z_{o1}=(L_1/C_1)^{1/2}$, $Z_{o2}=(L_2/C_2)^{1/2}$
Q_1, Q_2	quality factors of Tx and Rx resonator $Q_1=Z_{o1}/R_1$, $Q_2=Z_{o2}/R_2$
Q	geometric mean of Q_1 and Q_2

current, respectively. Circuit parameters used in the mathematical formulation are summarized in Table 1. It should be noted that the equivalent series resistance (ESR) such as R_1 or R_2 is the sum of individual ESR's in the coil as well as the compensation capacitor. By circuit analysis, the linear relation between the phasors can be obtained as

$$\begin{bmatrix} V_i/(R_s+R_1) \\ 0 \end{bmatrix} = \begin{bmatrix} -j\frac{Q_1}{1+R_s/R_1}\left(\omega_N - \omega_N^{-1}\right)+1 & j\omega_N k_1 \frac{Q_1}{1+R_s/R_1} \\ j\omega_N k_2 \frac{Q_2}{1+R_s/R_1} & -j\frac{Q_2}{1+R_L/R_2}\left(\omega_N - \omega_N^{-1}\right)+1 \end{bmatrix} \begin{bmatrix} I_1 \\ I_2 \end{bmatrix} \quad (1)$$

As it is necessary to simplify the subsequent formulation, three assumptions are made. First, transmitter and receiver energy links are symmetric: $L_1 = L_2 = L$, $C_1 = C_2 = C$, $R_1 = R_2 = R$, $k_1 = k_2 = k$, and $Q_1 = Q_2 = Q$. Secondly, switching devices are nearly ideal and thus the source impedance is small enough to be ignored: $R_s = 0$. Lastly, the operating frequency of the system is the same as the resonant frequency of the circuit, $\omega_N = 1$. Meanwhile, it is convenient to introduce two axis variables as in the following,

$$FOM \equiv kQ, \quad r_d \equiv \frac{R_L}{R}. \quad (2)$$

where the figure-of-merit (FOM) indicates the performance of the resonant link itself, and r_d is the ratio of the load resistance to the internal ESR of the resonant link.

Now, design equations are readily derived from (1). Power transfer efficiency of the resonant link is given by formula (3).

$$\eta = \frac{\frac{1}{2}R_L|I_2|^2}{\frac{1}{2}R_1|I_1|^2 + \frac{1}{2}R_2|I_2|^2 + \frac{1}{2}R_L|I_2|^2} = \frac{FOM^2 r_d}{(1+r_d)^2 + FOM^2(1+r_d)} \equiv f(r_d, FOM) \quad (3)$$

Similarly, AC voltage gain formula is formulated in (4).

$$M_{V,AC} \equiv \left|\frac{V_o}{V_i}\right| = \frac{\sqrt{R_L P_o}}{|V_i|} \approx \frac{FOM^2 r_d^2}{[FOM^2 + (1+r_d)]^2} \equiv g(r_d, FOM) \quad (4)$$

Because both (3) and (4) are functions of FOM and r_d, it is clear that these two new parameters can be used as design variables.

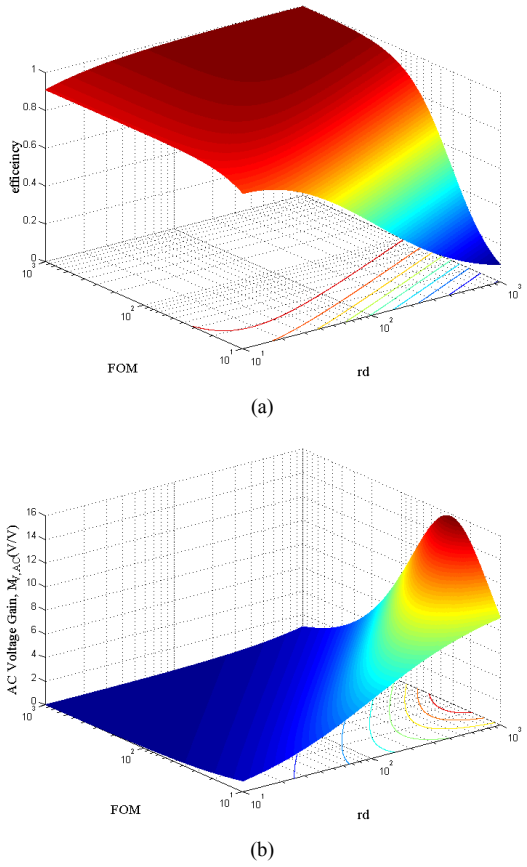

Fig. 3. Performance indices in FOM-r_d plane. (a) Efficiency. (b) Voltage gain.

Fig. 3 (a) and (b) are the surface plots in the FOM-r_d plane describing the efficiency and the voltage gain respectively. Fig. 4 is a contour plot representing the two performance indices on the same plane and thus is useful in the resonant link design.

B. Operating Point Analysis in the FOM-r_d Plane

It is possible to locate the operating point by directly calculating FOM and r_d for a ready-made energy link structure. In this case, the proposed FOM-r_d plane provides an intuitive way of understanding of the performance dependency on the external conditions such as degree of misalignment, coil distance, and the load resistance effects. For example, if the distance between Tx and Rx coils increases, degraded coupling coefficient makes the operating point move further downward as shown in Fig. 4. As a result, the efficiency will decrease and the voltage gain will increase. On the other hand, as the equivalent load resistance R_L increases, the operating point moves to the right as shown in Fig. 4, so that the efficiency will decrease and the voltage gain will increase.

Another advantage of the FOM-r_d plane analysis is that a peak splitting phenomenon called bifurcation can be graphically detected. The gain bifurcation makes a challenge in a frequency-controlled output regulation mechanism and sometimes hampers the soft-switching operation of the Tx inverter power switches. The criterion to prevent bifurcation from occurring in S-S configuration has been studied in [1], [8], and is

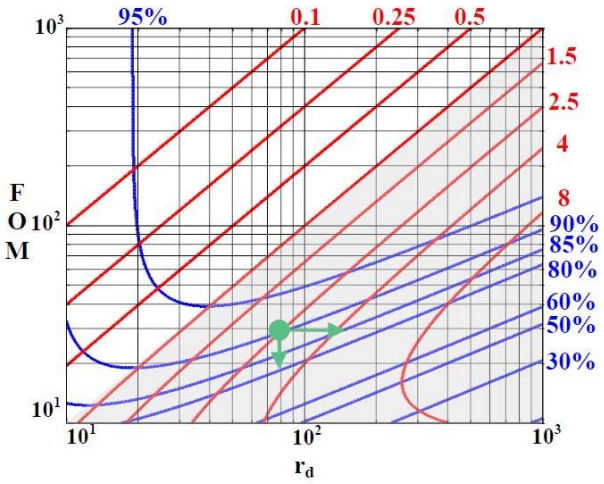

Fig. 4. FOM-r_d design plane.

$$k < \frac{Z_{o2}}{R_2 + R_L}. \tag{5}$$

This inequality can be rewritten for the design space, FOM-r_d plane, as shown in (6).

$$FOM < 1 + r_d \tag{6}$$

It is clear that the above condition to guarantee the bifurcation-free operation can be mapped into the lower right shaded region in Fig. 4.

C. Energy Link Design in FOM-r_d Plane

The FOM-r_d plane is convenient, especially for the energy link design process. An energy link can be designed by locating one operating point on the design plane through target efficiency and voltage gain. Thereafter, with additional conditions such as the coupling coefficient, the load resistance, and the resonant frequency, all the circuit parameters for the resonant energy link can be calculated by the following equations.

$$Q = \frac{FOM}{k},\ R = \frac{R_L}{r_d},\ L = \frac{QR}{\omega_o},\ C = \frac{1}{QR\omega_o} \tag{7}$$

As mentioned before, as the system approaches to the full load condition, the operating point tends to move further into the region of bifurcation. Likewise, as the degree of coil misalignment or the distance between coils decreases, the energy link becomes more prone to the bifurcation. Therefore, it is necessary to start the design in the full load and the maximum coupling coefficient in order to guarantee the uniqueness of the voltage gain peak.

III. Verification of The Proposed Method

A. Design Example

In this section, a 200 W energy link structure for the IPT system in Fig. 2 has been designed for verifying FOM-r_d plane.

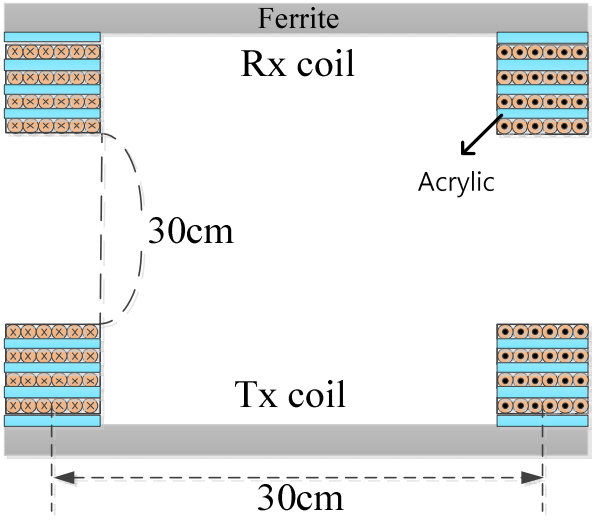

Fig. 5. Shape of coils for resonant link design.

The target voltage gain is calculated as 2.5 from the voltage specification, $V_{i,DC}$ = 80 V and $V_{o,DC}$ = 200 V. The effective load resistance, R_L is calculated as 40.5 Ω from the output power rating.

According to Fig. 4, along the line of $M_{V,AC}$=2.5, energy link with larger values in both FOM and r_d shows higher power transfer efficiency, but the maximum achievable efficiency is usually limited by the ESR of resonators. The target efficiency is set to 90 %. By the FOM–r_d plane in Fig. 4, FOM = 28 and r_d = 78 are selected to meet the specification. When the magnetic coupling factor, k, is assumed to be 0.04 and the resonant frequency of the system, ω_o, is set to 100 kHz, the circuit parameters are calculated as Q = 700, R = 519 mΩ, L = 579 uH, and C = 4.37 nF using (7). Through the equivalent circuit mode Tx-side capacitor shows the voltage stress and the current stress of 3.2 kV and 8.8 A in magnitude, and Rx-side capacitor goes through the voltage stress and the current stress of 1.1 kV and 3.1 A in magnitude, respectively.

B. Experimental Results

For the implementation of resonant capacitors is performed. The capacitor bank structure consists of series as well as parallel connection, because the voltage and current stresses of Tx-side capacitor must be considered. As a result, high voltage film capacitors (ICEL, PSB2301680KGS) are used in 6S-4P configuration. According to the capacitor datasheet, this component has 6.8 nF capacitance that endures 750 V (RMS), and ESR of the capacitor at 100 kHz is found to be 64 mΩ. Thus capacitor bank totally carries 4.53 nF capacitance with 96 mΩ ESR and withstands as high as 4.5 kV (RMS). The same configuration has been used for Rx-side capacitor bank.

On the other hand, Fig. 5 shows the coil winding configuration. Coils used in this paper are formed by spiral windings with square cross section. They have 30 cm mean coil diameter and are appended by 30 cm x 30 cm x 0.5 cm square ferrite plate. Since the voltage stress in the coil is also quite high with 3.2 KV, acrylic insulation layers to avoid electrical breakdown between windings are inserted. To make the mutual

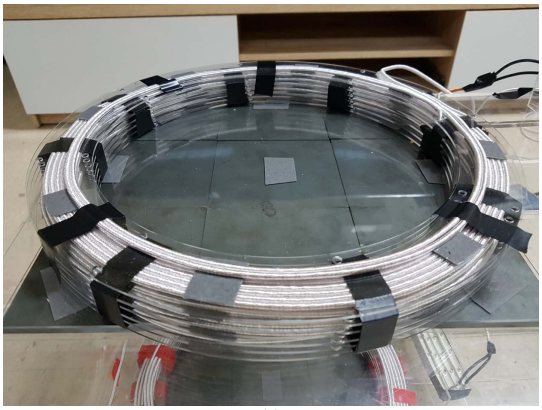

(a)

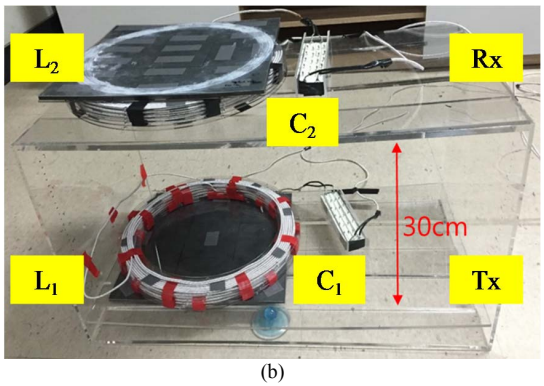

(b)

Fig. 6. Implementation of (a) Rx coil and (b) resonant link.

inductance to be k = 0.04, Tx and Rx coils have placed apart with the distance of 30 cm, which has been assisted by the finite element analysis (FEA) using FEMM v4.2 and then slightly adjusted experimentally.

The inductance formula in [9] has been utilized for implementing the practical coil structure whose value of inductance is 579 uH. The inductance calculation has been carried out by Stefan's formula,

$$S(r,N) = 4\pi\left[\frac{1}{2}\left\{1+\frac{1}{6}\left(\frac{b}{2a}\right)^2\right\}ln\frac{8}{\left(\frac{b}{2a}\right)^2} - 0.84834 + 0.2041\left(\frac{b}{2a}\right)^2\right], \quad (4)$$

$$L = 0.1aN^2S(r,N) \quad [\text{uH}]. \quad (9)$$

where the value of a, b, r and N represents the mean radius in cm, length of coil cross section in cm, conductor size in mm and the number of turns, respectively.

It is important to consider the ESR of coils together with ESR of capacitors. The target ESR value of coil is obtained as 423 mΩ from subtracting the ESR of the capacitor bank from the total ESR value. Even though the wire resistance increases far larger than the DC static resistance with high frequency operation, adopting Litz-wire for suppressing skin effect will lead to a moderate rise in the resistance. Analysis of the AC resistance by proximity and skin effect has been partially assisted by the

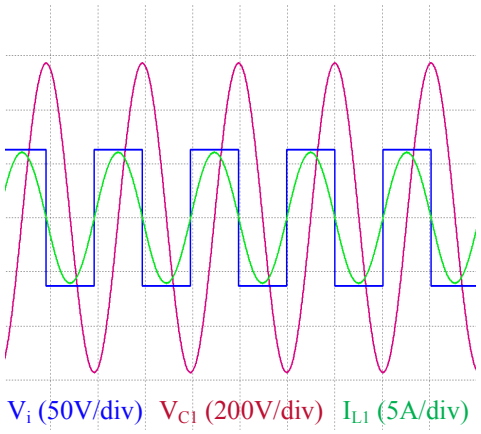

(a)

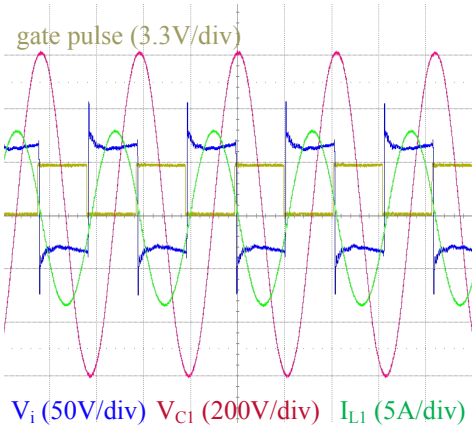

(b)

Fig. 7. Experimental results. (a) Simulation Waveforms (5us/div). (b) Hardware Waveforms (5us/div).

FEA as well as the experimental results Considering the margin accounting for the proximity effect, the target DC resistance is empirically designed to be 200 mΩ using the formula given in (10).

$$R_{DC}(r,N) = 2\rho\frac{aN}{r^2} \quad [\Omega] \quad (10)$$

As a result, the coils have been made by Litz-wire with 1.2 mm diameter and 30 turns, (N = 30) The implemented coil and the resonant energy link made up of designed capacitor banks and coils are shown in Fig. 6 (a) and (b), respectively.

The overall system which contains the resonant link has been tested with a full-bridge inverter for Tx-side, and a passive rectifier for Rx-side that has the same structure with the inverter. Fig. 7 (a) and (b) show LTSPICE simulation and hardware waveforms respectively, and two operating waveforms match well with each other. When the input power is 231.9 W (46.15 V, 5.03 A), the output power is measured to be 182.80 W (95.6 V, 1.92 A), and thus the overall DC to DC efficiency of the IPT system is 78.8 %. To aid the efficiency analysis, PLECS thermal simulation considering the device datasheet shows the inverter efficiency and the rectifier efficiency are 98.1 %, and 98 %, and thus the energy link

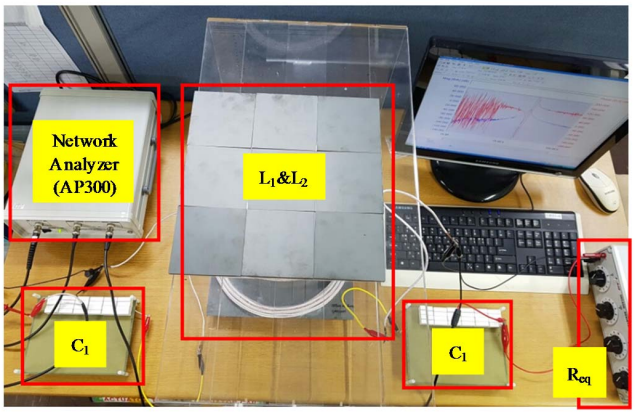

(a)

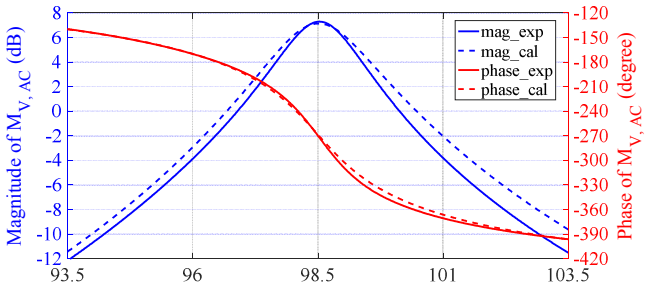

(b)

Fig. 8. Frequency analysis experimental (a) set up and (b) the voltage gain and phase comparison results.

efficiency is estimated to be 85 %. The actual measurement of the voltage gain in the resonant link is 2.32.

For further comparisons, some other measurements have been made. The LCR meter (Agilent, 4263B) reading says that the capacitance and the self-inductance are 4.12 nF and 633 uH. Using the impedance measurement set-up with AP Instruments, AP300 in Fig. 8 (a), Tx-side total ESR is measured to 0.76 Ω at the resonant frequency of 98.52 kHz. From these observations, the actual energy link design point has been slightly moved to (FOM, r_d) = (20.7, 53), which indicates the implemented efficiency and the voltage gain to be 87 % and 2.27, respectively. Fig. 8 (b) shows the magnitude-phase comparisons of the voltage gain and the measurement results matches well with the simulation.

IV. Conclusion

This paper presents a new graphical method based on FOM-r_d plane that can intuitively describe the energy link of the IPT system. Using the proposed method, the voltage gain as well as the efficiency can be designed together in terms of power conversion circuit. In addition, it is easy to estimate the performance and to check the bifurcation condition even with perturbations in the magnetic coupling or in the system load. By applying the proposed design method, a 200 W energy link system has been successfully constructed. The validity of the design is verified by comparing the simulation and the hardware results, and the differences are about 2.0 % in the efficiency and about 2.2 % in the voltage gain. To conclude, the suggested method is expected to provide a powerful methodology for both analysis and design of IPT system.

References

[1] Chwei-Sen Wang, G. A. Covic and O. H. Stielau, "Power transfer capability and bifurcation phenomena of loosely coupled inductive power transfer systems," in *IEEE Transactions on Industrial Electronics*, vol. 51, no. 1, pp. 148-157, Feb. 2004.

[2] J. Sallan, J. L. Villa, A. Llombart and J. F. Sanz, "Optimal Design of ICPT Systems Applied to Electric Vehicle Battery Charge," *IEEE Trans. Ind. Electron.*, vol. 56, no. 6, pp. 2140-2149, June 2009.

[3] S. Chopra and P. Bauer, "Analysis and design considerations for a contactless power transfer system," in *Proc. IEEE 33rd INTELEC*, 2011, pp. 1-6.

[4] S. Raju, R. Wu, M. Chan and C. P. Yue, "Modeling of mutual coupling between planar inductors in wireless power applications," *IEEE Trans. Power Electron.*, vol. 29, no. 1, pp. 481-490, Jan. 2014.

[5] T. Komaru, M. Koizumi, K. Komurasaki, T. Shibata and K, Kano, "Parametric evaluation of mid-range wireless power transmission," *2010 IEEE International Conference on Industrial Technology*, Vi a del Mar, 2010, pp. 789-792.

[6] H. Sugiyama, "Optimal designs for wireless resonant energy link with symmetrical coil pair," *2011 IEEE MTT-S International Microwave Workshop Series on Innovative Wireless Power Transmission: Technologies, Systems, and Applications*, Uji, Kyoto, 2011, pp. 247-250.

[7] W. Zhang, S. C. Wong, C. K. Tse and Q. Chen, "Design for efficiency optimization and voltage controllability of series−series compensated inductive power transfer systems," *IEEE Trans. Power Electron.*, vol. 29, no. 1, pp. 191-200, Jan. 2014.

[8] P. E. K. Donaldson, "Frequency-hopping in r.f. energy-transfer links," *Electron. & Wireless World*, pp. 24-26, Aug. 1986.

[9] Frederick Warren Grover, *Inductance Calculations: Working Formulas and Tables*, Van Nostrand, New York, 1946.